Polarization-dependent tunneling of light in gradient optics

A. Shvartsburg,[1] V. Kuzmiak,[2] and G. Petite[3]
[1]*Science Technology Center for Unique Instrumentation, Russian Academy of Sciences, P.O. Box 117342, Butlerov Street 15, Moscow, Russia*
[2]*Institute of Radio Engineering and Electronics, Czech Academy of Sciences, Chaberska 57, 182 51 Praha 8, Czech Republic*
[3]*Laboratoire des Solides Irradies, Ecole Polytechnique, CEA—DSM, CNRS, 91128, Palaiseau, France*
(Received 13 July 2006; published 12 July 2007)

Reflection-refraction properties of photonic barriers, formed by dielectric gradient nanofilms, for inclined incidence of both *S*- and *P*-polarized electromagnetic waves are examined by means of exactly solvable models. We present generalized Fresnel formulas, describing the influence of the nonlocal dispersion on the reflectance and transmittance of single- and double-layer gradient photonic barriers for *S* and *P* waves and arbitrary angles of incidence. The nonlocal dispersion of such layers, arising due to a concave spatial profile of dielectric susceptibility across the plane film, is shown to result in a peculiar heterogeneity-induced optical anisotropy, providing the propagation of *S* (*P*) waves in tunneling (traveling) regimes. The results obtained indicate the possibility of narrow-band nonattenuated tunneling (complete transmittance) of oblique *S* waves through such heterogeneous barriers, and the existence of spectral areas characterized by the strong reflection of *P* waves and profound contrast between transmitted *S* and *P* waves. The scalability of obtained exact analytical solutions of Maxwell equations into the different spectral ranges is discussed and the application potential of these phenomena for miniaturized polarizers and filters is demonstrated.

DOI: 10.1103/PhysRevE.76.016603 PACS number(s): 42.25.Bs

I. INTRODUCTION

Tunneling is a basic wave phenomenon with many interesting applications. The concept of tunneling was pioneered by Gamow for particles in quantum mechanics as long ago as in 1928 [1]. Later on both the quantum approach, involving the time-independent Schrodinger equation, and the wave approach, involving the Helmholtz monochromatic wave equation, were considered to be formally equivalent. The advent of lasers has attracted attention to the effects associated with tunneling of the electromagnetic (EM) waves through classical barriers in a series of optoelectronic problems such as, e.g., the evanescent modes in dielectric waveguides [2] and liquid crystals [3], and the Goos-Hanchen effect for curvilinear interfaces [4–6]. Experiments in the microwave range with an "undersized" waveguide [7], and the Goos-Hanchen spatial shift of a narrow beam, passing through paraffine double prisms [8], have demonstrated the possibilities of observation of tunneling effects, which proved not to be easy to reproduce at quantum scales. Side by side with the numerous applications of the tunneling concept in optoelectronics, solid state, and microwave physics [9], this concept contains an intriguing theoretical challenge, connected with the idea of superluminal light tunneling through the photonic barrier known as the Hartman paradox [10,11].

The theoretical background of the aforesaid investigation is based on the electromagnetics of heterogeneous media [12]. Herein some important features of evanescent waves are examined usually in the framework of a simple model of a rectangular opaque barrier [13] or layered structure, formed by steplike variations of refractive indices [14]. Another field for wave-tunneling phenomena is connected with the gradient optics of thin films: the nonlocal dispersion, arising due to continuous spatial variations of dielectric susceptibility was shown recently to provide a rich variety of tunneling phenomena even in a material with negligible natural local dispersion [15]. These phenomena can be examined by means of exact analytical solutions of Maxwell equations for media with spatially distributed dielectric susceptibility

$$\varepsilon(z) = n_0^2 U^2(z). \tag{1}$$

Here n_0 is the value of the host dielectric refractive index; the dimensionless function $U(z)$ describes the coordinate dependence of the dielectric susceptibility. This heterogeneity can result in the formation of a cutoff frequency Ω, dependent on the gradient and curvature of the $\varepsilon(z)$ profile [15]. Thus, for heterogeneous nanofilms with a thickness of about 100 nm and with a depth of modulation of refractive index about 25% the cutoff frequencies Ω, separating the evanescent and traveling modes, belong to the near IR or visible spectral ranges. Controlled variety of reflection-refraction properties of the layer, produced by different profiles $U(z)$, opens new possibilities of designing of media with optical properties unattainable in natural materials.

The role of the heterogeneity-induced dispersion was examined in Ref. [15] for the case of normal incidence, when the wave-polarization effects are vanishing; however, the model $U(z)$ used in Ref. [15] does not provide analytical solutions of the wave equation in the inclined incidence case. Unlike Ref. [15], this paper is devoted to the peculiar effects in the reflectivity and transmittivity of both *S*- and *P*-polarized waves, incidenting under an arbitrary angle on an heterogeneous dielectric layer, characterized by some profile $U(z)$.

The paper is organized as follows. In Sec. II we present a model of nonmonotonic concave profile $U(z)$, suitable for both *S* and *P* waves in the gradient medium and demonstrate the effects of heterogeneity-induced optical anisotropy. Exact

analytical solutions of the wave equations obtained for such $U(z)$, revealing the polarization-dependent propagation and tunneling regimes for both one- and two-gradient layers, are examined in Sec. III. In Sec. IV we use these solutions for the analysis of narrow-band reflectionless tunneling of S waves, the strong reflection of P waves, the deep contrast between transmitted S and P waves, and some phase effects, associated with the aforesaid phenomena. The conclusions are summarized in Sec. V.

II. PROPAGATION AND TUNNELING OF S- AND P-POLARIZED WAVES IN GRADIENT MEDIA (EXACTLY SOLVABLE MODEL)

Unlike in the case of the normal incidence, here the waves have a different polarization structure and are described by different equations. By denoting the normal to the layer as the z axis and choosing the projection of the wave vector on the layer's interface as the y axis, one can describe the polarization structure of an S wave by means of its electric component E_x and the magnetic components H_y and H_z. The layer is assumed to be lossless and nonmagnetic, and one can write the Maxwell equations linking these components as

$$\frac{\partial E_x}{\partial z} = -\frac{1}{c}\frac{\partial H_y}{\partial t}, \quad \frac{\partial E_x}{\partial y} = \frac{1}{c}\frac{\partial H_z}{\partial t}, \quad \frac{\partial H_z}{\partial y} - \frac{\partial H_y}{\partial z} = \frac{\varepsilon(z)}{c}\frac{\partial E_x}{\partial t}, \tag{2}$$

$$\mathrm{div}(\varepsilon \bar{E}) = 0, \quad \mathrm{div}(\bar{H}) = 0. \tag{3}$$

Components of the P wave (H_x, E_y, and E_z) also satisfy Eqs. (3), however Eqs. (2) are in this case replaced by

$$\frac{\partial H_x}{\partial z} = \frac{\varepsilon(z)}{c}\frac{\partial E_y}{\partial t}, \quad \frac{\partial H_x}{\partial y} = -\frac{\varepsilon(z)}{c}\frac{\partial E_z}{\partial t}, \quad \frac{\partial E_z}{\partial y} - \frac{\partial E_y}{\partial z} = -\frac{1}{c}\frac{\partial H_x}{\partial t}. \tag{4}$$

The effects of heterogeneity-induced dispersion for inclined incidence can be found from the set of Eqs. (2)–(4) by means of exactly solvable models of $\varepsilon(z)$ given by Eq. (1), suitable for both S and P polarizations. The well-known Rayleigh profile $U(z)=(1+z/L)^{-1}$, dating back to 1880, and the exponential profile $U(z)=\exp(\pm z/L)$ provide exact solutions of the set of equations (2)–(4) for monotonic variations of $U(z)$ [12]; however, these models are not suitable for the description of smoothly varying concave photonic barriers, which we plan to discuss. Thus, the reflection-refraction problem for the set of equations (2)–(4) is considered below from the very beginning. It is convenient to express the field components in Maxwell equations by means of the following auxiliary, polarization-dependent functions Ψ_s and Ψ_p:

$$S \text{ polarization:} \quad E_x = -\frac{1}{c}\frac{d\Psi_s}{dt}, \quad H_y = \frac{d\Psi_s}{dz}, \quad H_z = -\frac{d\Psi_s}{dy}, \tag{5}$$

$$P \text{ polarization:} \quad H_x = -\frac{1}{c}\frac{d\Psi_p}{dt}, \quad E_y = \frac{1}{\varepsilon(z)}\frac{d\Psi_p}{dz},$$

$$E_z = -\frac{1}{\varepsilon(z)}\frac{d\Psi_p}{dy}. \tag{6}$$

Using such representations one can reduce the system [Eqs. (2)–(4)] to two equations, governing S and P waves, respectively. Omitting for simplicity the factor $\exp[i(k_y y-\omega t)]$, these equations can be written as

$$\frac{\partial^2 \Psi_s}{\partial z^2} + \left(\frac{\omega^2 n_0^2 U^2}{c^2} - k_y^2\right)\Psi_s = 0, \quad k_y = \frac{\omega}{c}\sin\theta, \tag{7}$$

$$\frac{\partial^2 \Psi_p}{\partial z^2} + \left(\frac{\omega^2 n_0^2 U^2}{c^2} - k_y^2\right)\Psi_p = \frac{2}{U}\frac{dU}{dz}\frac{\partial \Psi_p}{\partial z}. \tag{8}$$

By introducing the new variable η and the new functions f_s and f_p,

$$\eta = \int_{z_0}^{z} U(z_1)dz_1, \quad f_s = \Psi_s\sqrt{U(z)}, \quad f_p = \frac{\Psi_p}{\sqrt{U(z)}}, \tag{9}$$

where z_0 denotes the position of the film or vacuum first interface, one can present Eqs. (7) and (8) for S and P waves in the forms

$$\frac{d^2 f_s}{d\eta^2} + f_s\left(\Lambda - \frac{U_{\eta\eta}}{2U} + \frac{U_\eta^2}{4U^2}\right) = 0, \tag{10}$$

$$\frac{d^2 f_p}{d\eta^2} + f_p\left(\Lambda + \frac{U_{\eta\eta}}{2U} - \frac{3U_\eta^2}{4U^2}\right) = 0, \tag{11}$$

where $\Lambda=(\omega^2 n_0^2/c^2)-(k_y^2/U^2)$, $U_\eta=dU/d\eta$, and $U_{\eta\eta}=d^2U/d\eta^2$. Equations (10) and (11) are valid for arbitrary profiles of photonic barriers $U(z)$ and all angles of incidence θ, including, in particular, the two well-known exactly solvable models mentioned above: the Rayleigh and exponential profiles. The fact that some polarization effects will depend on the barrier profile is clear even without a solution of these equations. In the case of the widely used Rayleigh profile U_R, which can be rewritten in η space by means of Eq. (9) as $U_R(\eta)=\exp(-\eta/L)$, both Eqs. (10) and (11) coincide:

$$\frac{d^2 f_{s,p}}{d\eta^2} + f_{s,p}\left(\frac{\omega n_0}{c}\right)^2\left[1 - \frac{\omega_{cr}^2}{\omega^2} - \frac{\sin^2\theta}{n_0^2}\exp\left(\frac{2\eta}{L}\right)\right] = 0. \tag{12}$$

Equation (12) shows that, due to heterogeneity-induced dispersion, characterized by a cutoff frequency $\omega_{cr}=c/2n_0L$, the tunneling regimes arise in the Rayleigh barrier for both S and P waves simultaneously. In the case of the exponential profile, rewritten in η space as $U=1\pm\eta/L$, no heterogeneity-induced cutoff frequency can be defined from Eqs. (10) and (11). In contrast to these traditionally used asymmetrical profiles, we consider here the exactly solvable symmetrical concave barrier $U(z)$, formed inside the dielectric film with the thickness d by variation of U from the value $U=1$ in the center of the barrier ($z=0$) up to the values U_m at the interfaces $z=\pm d/2$ (Fig. 1 represents the case of a system consisting of two such barriers deposited on a substrate with the constant refractive index n_D),

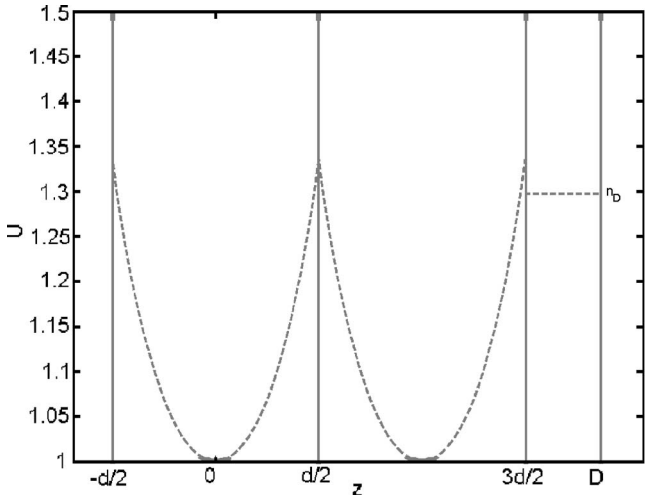

FIG. 1. Pair of gradient layers, supported by an homogeneous substrate; the thickness of each layer and substrate are d and D, respectively; the profile of the refractive index inside each gradient layer is described by Eq. (13).

$$U = \frac{1}{\cos\left(\frac{z}{L}\right)}, \quad U_m = \frac{1}{m}, \quad m = \cos\left(\frac{d}{2L}\right). \tag{13}$$

With these conventions, the integral in Eq. (9) should be taken from $z_0 = -d/2$. Note that this model is characterized by one free parameter—the length scale L, however, it can be used to study many features associated with this type of potential as we will show in Sec. IV. In fact, it represents a particular case of a more general potential with two adjustable parameters which, however, leads to much more cumbersome calculations and thus is not developed here. By substituting Eq. (13) into Eq. (9) one can express the profile $U(\eta))$ in terms of the new variable η,

$$\eta = L \ln\left[\frac{1 + tg(z/2L)}{1 - tg(z/2L)}\right], \quad U = \frac{1}{\cos\left(\frac{z}{L}\right)} = ch\xi, \quad \xi = \frac{\eta}{L}. \tag{14}$$

By using Eq. (14) one can rewrite Eqs. (10) and (11) for S and P waves inside the barrier given by Eq. (13) into the similar form,

$$\frac{d^2 f_{s,p}}{d\xi^2} + f_{s,p}\left(q^2 - \frac{\Gamma_{s,p}}{ch^2\xi}\right) = 0, \tag{15}$$

$$q^2 = \left(\frac{\omega n_0 L}{c}\right)^2 \left(1 - \frac{\Omega^2}{\omega^2}\right), \tag{16}$$

$$\Gamma_s = (k_y L)^2 + \frac{1}{4}, \quad \Gamma_p = (k_y L)^2 - \frac{3}{4}, \tag{17}$$

where Ω is a characteristic frequency, determined by the parameters of concave barrier (13),

$$\Omega = \frac{c}{2n_0 L} = \frac{c}{n_0 d} \arccos(m). \tag{18}$$

The sign of parameter q^2 given by Eq. (16) changes in $\omega = \Omega$. Let us consider here the low-frequency spectral range $\omega < \Omega$, $q^2 < 0$. In this range the expression in brackets in Eq. (15) for the S wave is always negative, and thus the low-frequency S wave, incidenting on the barrier given by Eq. (13) under an arbitrary angle θ, is traversing this barrier as an evanescent wave. On the contrary, the same expression in Eq. (15) for a P wave, for realistic values of the modulation of the refractive index (13) in the layer ($U_m = m^{-1} \leqslant 1.3-1.4$) remains positive and provides the traveling-mode regime for the P wave.

Thus, unlike the homogeneous rectangular barrier, where the tunneling of the EM waves is determined by a condition common to both S and P polarizations, the tunneling through the concave barrier given by Eq. (13) proves to be polarization dependent. This heterogeneity-induced anisotropy can result in a significant difference in reflectivity and transmittivity of such a barrier for S and P waves, with their frequencies and angles of incidence on the layer being equal. This difference is illustrated below by means of the exactly solvable model (13).

III. HETEROGENEITY-INDUCED OPTICAL ANISOTROPY OF TRANSPARENT LAYERS

To simplify the analysis of the transmission of a concave photonic barrier for the EM wave with inclined incidence, let us first consider one layer without a substrate embedded in free space (see Fig. 1). We introduce the dimensionless quantities

$$u = \Omega/\omega > 1, \quad N = \sqrt{1 - u^{-2}} < 1. \tag{19}$$

By transforming Eq. (15) by means of the new variable ν and the new function W,

$$\nu = \frac{1 - th\xi}{2}, \quad f_{s,p} = (ch\xi)^{N/2} W_{s,p}, \tag{20}$$

one obtains for this function the hypergeometric equation

$$\nu(1-\nu)\frac{d^2 W}{d\nu^2} + [\gamma - \nu(1 + \alpha + \beta)]\frac{dW}{d\nu} - \alpha\beta W = 0,$$

$$\gamma = 1 - \frac{N}{2}. \tag{21}$$

Although Eq. (21) is valid for both polarizations, the values of parameters α and β have to be specified for each wave, while the definition γ given by Eq. (21) is valid for both waves. Let us start the analysis from the S wave; in this case

$$\alpha_s, \beta_s = \frac{1}{2}\left[1 - N \pm \frac{i \sin\theta\sqrt{1 - N^2}}{n_0}\right]. \tag{22}$$

Since $\alpha_s + \beta_s + 1 = 2\gamma$, two linearly independent solutions of Eq. (21) are given by the hypergeometric functions $F(\alpha_s, \beta_s, \gamma, \nu)$ and $F(\alpha_s, \beta_s, \gamma, 1-\nu)$, denoted below for com-

pactness as $F(\nu)$ and $F(1-\nu)$; moreover, due to condition $\mathrm{Re}(\alpha_s+\beta_s-\gamma)<0$ the series, presenting these functions, are converging absolutely [16]. The general solution of Eq. (21) reads as

$$W = F(\nu) + Q_s F(1-\nu). \tag{23}$$

Here $F(\nu)$ and $F(1-\nu)$ can be considered as forward and backward waves (meaning more exactly in a tunneling case, evanescent and antievanescent waves), while the factor Q_s is associated with the contribution of backward wave to the total field. By using the variables defined in Eqs. (9) and (19) and expressing the factor ch ξ in terms of $\cos(z/L)$ according to Eq. (14), one can present the generating function Ψ_s in the form

$$\Psi_s = [\cos(z/L)]^{(1-N)/2} W. \tag{24}$$

The substitution of Eq. (24) into Eq. (5) yields the explicit expressions for components of the S wave inside the medium,

$$E_x = \frac{i\omega A}{c}\Psi_s, \quad H_z = -ik_y A \Psi_s,$$

$$H_y = \frac{-A}{2L[\cos(z/L)]^{(N+1)/2}}\left\{(1-N)\sin(z/L)W + \cos^2(z/L)\frac{dW}{d\nu}\right\}, \tag{25}$$

where A is the complex amplitude of the wave. To find the reflection coefficient for the S wave R_s one has to use the continuity conditions on the film interfaces $z=\pm d/2$. It follows from Eq. (14) that

$$th\xi = \sin(z/L), \quad \nu = \frac{1-\sin(z/L)}{2}, \quad 1-\nu = \frac{1+\sin(z/L)}{2}. \tag{26}$$

Let us consider the wave incidenting on the interface $z=-d/2$. By introducing the variables $\nu_{1,2}$,

$$\nu|_{z=-d/2} = \nu_1 = \frac{1+s}{2}, \quad (1-\nu)|_{z=+d/2} = \nu_2 = \frac{1-s}{2},$$

$$s = \sqrt{1-m^2},$$

$$F_{1,2} = F(\nu_{1,2}), \quad F_1' = \left.\frac{dF}{d\nu}\right|_{\nu_1}, \quad F_2' = \left.\frac{dF}{d\nu}\right|_{\nu_2}. \tag{27}$$

Using the values of field components (25) on the interface $z=-d/2$ and omitting, for simplicity, here and below the phase factors $\exp[i(k_y y-\omega t)]$, one can derive the expression for R_s from the continuity conditions on this interface,

$$R_s = \frac{M_1 + i\zeta_s F_1 + Q_s(M_2 + i\zeta_s F_2)}{i\zeta_s F_1 - M_1 + Q_s(i\zeta_s F_2 - M_2)}, \tag{28}$$

$$M_{1,2} = s(N-1)F_{1,2} \pm m^2 F_{1,2}', \quad \zeta_s = \frac{m\cos\theta\sqrt{1-N^2}}{n_0}. \tag{29}$$

The factor Q_s can be determined in the same way from the continuity conditions on the opposite interface $z=d/2$,

$$Q_s = -\left(\frac{M_2 - i\zeta_s F_2}{M_1 - i\zeta_s F_1}\right). \tag{30}$$

By substituting Q_s given by Eq. (30) into Eq. (28) one obtains the complex reflection coefficient R_s,

$$R_s = \frac{A_s}{B_s}, \quad A_s = M_1^2 - M_2^2 + \zeta_s^2(F_1^2 - F_2^2), \quad B_s = B_1 + iB_2,$$

$$B_1 = M_2^2 - M_1^2 + \zeta_s^2(F_1^2 - F_2^2), \quad B_2 = 2\zeta_s(F_1 M_1 - F_2 M_2). \tag{31}$$

Now we rewrite the complex reflection coefficient R_s into the form $R_s = |R_s|\exp(i\phi_{sr})$,

$$|R_s| = \frac{|A_s|}{\sqrt{B_1^2 + B_2^2}}, \quad \phi_{sr} = -\arctan\left(\frac{B_2}{B_1}\right). \tag{32}$$

To find the transmission function T_s we express the amplitude of the refracted wave A from Eq. (25) in terms of the amplitude of the incidenting wave E_0 and the reflection coefficient R_s,

$$A = \frac{-iE_0 c(1+R_s)}{\omega(F_1 + Q_s F_2)}. \tag{33}$$

By using Eq. (33) one can write the field E at the interface $z=d/2$ by means of a complex transmission function T_s,

$$E = E_0 T_s, \quad T_s = |T_s|\exp(i\phi_{st}),$$

$$|T_s| = \frac{2\zeta_s|F_1 M_2 - F_2 M_1|}{\sqrt{B_1^2 + B_2^2}}, \quad \phi_{st} = \arctan\left(\frac{B_1}{B_2}\right). \tag{34}$$

The reflection coefficient for the P wave R_p can be calculated in the same way. The generating function Ψ_p [Eq. (6)] is expressed via the relevant solution of Eq. (21), similar to Eq. (23),

$$\Psi_p = [\cos(z/L)]^{-(N+1)/2}[F(\alpha_p, \beta_p, \gamma, \nu) + Q_p F(\alpha_p, \beta_p, \gamma, 1-\nu)],$$

$$Q_p = -\left(\frac{M_4 - i\zeta_p F_4}{M_3 - i\zeta_p F_3}\right),$$

$$\zeta_p = \frac{n_0\cos\theta\sqrt{1-N^2}}{m}. \tag{35}$$

Forward and backward (propagating) waves are described by Eq. (35) in terms of the hypergeometric functions F with parameters

$$\alpha_p,\beta_p=\frac{1}{2}\left[1-N\pm\sqrt{4-\frac{(1-N^2)\sin^2\theta}{n_0^2}}\right],\quad \gamma=1-\frac{N}{2}. \tag{36}$$

By substituting the generating function given by Eq. (35) into Eq. (6) one obtains the components of the P wave. Using the continuity conditions, one can present the reflection coefficient R_p in a form, analogous to R_s [Eq. (32)].

$$R_p=\frac{M_3+i\varepsilon_pF_3+Q_p(M_4+i\varepsilon_pF_4)}{i\varepsilon_pF_3-M_3+Q_p(i\varepsilon_pF_4-M_4)},$$

$$R_p=|R_p|\exp(i\phi_{pr}),\quad |R_p|=\frac{|A_p|}{\sqrt{B_3^2+B_4^2}},\quad \phi_{pr}=-\arctan\left(\frac{B_4}{B_3}\right),$$

$$A_p=M_3^2-M_4^2+\varepsilon_p^2(F_3^2-F_4^2),$$

$$B_3=M_4^2-M_3^2+\varepsilon_p^2(F_3^2-F_4^2),\quad B_4=2\varepsilon_p(F_3M_3-F_4M_4),$$

$$M_{3,4}=s(N+1)F_{3,4}\pm m^2F'_{3,4},$$

$$F'_{3,4}=\left.\frac{dF(\alpha_p,\beta_p,\gamma,\nu)}{d\nu}\right|_{\nu=\nu_{1,2}}. \tag{37}$$

The transmission function for the P wave T_p can be found by analogy with Eqs. (33) and (34) in the form

$$T_p=|T_p|\exp(i\phi_{pt}),$$

$$|T_p|=\frac{2\zeta_p|F_3M_4-F_4M_3|}{\sqrt{B_3^2+B_4^2}},\quad \phi_{pt}=\arctan\left(\frac{B_3}{B_4}\right). \tag{38}$$

Thus, we found the expressions for reflection coefficients $R_{s,p}$ and transmission functions $T_{s,p}$, valid for an arbitrary angle of incidence θ. The quantities $|R_{s,p}|$ and $|T_{s,p}|$ are linked by the energy conservation law,

$$|T_{s,p}|^2=1-|R_{s,p}|^2. \tag{39}$$

It is worth emphasizing that in the normal incidence case ($\theta=0$) the difference between S- and P-polarized waves vanishes, and thus the modules of reflection and transmission coefficients have to be equal. This equality, which is not obvious from the formulas for $|R_s|$ [Eq. (32)] and $|R_p|$ [Eq. (37)], is demonstrated in the Appendix. Therein we show that the field expressions for S and P waves inside the film coincide in this case, as it should, and hence all the derived quantities.

The effects of heterogeneity-induced dispersion on the amplitude-phase structure of transmitted radiation manifest themselves, first of all, by the angular dependence of the transmittance of gradient layers for S- and P-polarized waves. These transmittances, $|T_s|^2$ and $|T_p|^2$, calculated by using Eqs. (34) and (38), respectively, are depicted in Fig. 2. In the case of inclined incidence $|T_p|^2$, exceeding $|T_s|^2$ can even reach the value $|T_p|^2=1$, illustrating the Brewster effect for a gradient layer. The angle θ, however, which is related to this reflectionless regime, differs from the Brewster angle θ_B for an homogeneous layer ($tg\,\theta_B=n_0$).

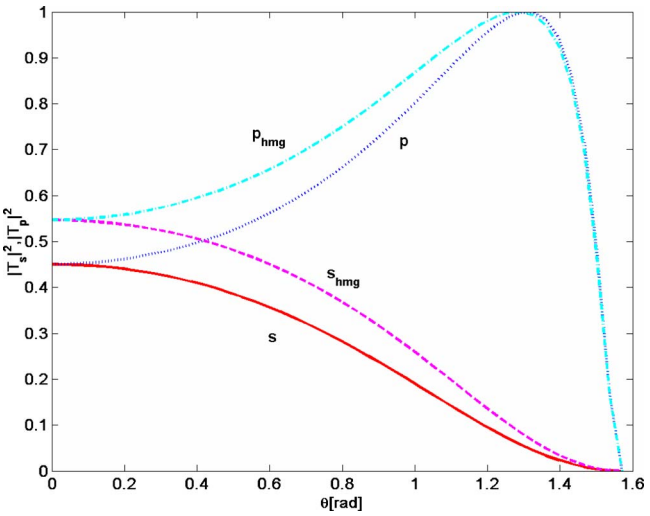

FIG. 2. (Color online) Transmittance vs the angle of incidence θ of both the gradient and homogeneous layer with parameters $m=0.75$, $n_0=3.4$, and $\gamma(u)=0.75$. Transmittances of the gradient layer for S and P waves are indicated by full and dotted lines, respectively, while transmittances associated with the homogeneous layer for S and P waves are indicated by a dashed and a dash-dotted line.

In Fig. 2 we present the angular dependence of transmittances of an heterogeneous layer for S and P waves for some given value of dimensionless parameter γ given by Eq. (21), defined for any normalized frequency $u=\Omega/\omega$. Considering the transmittance regime, related to some values γ, m, θ, and n_0 and using the characteristic frequency Ω given by Eq. (18), one can choose the thickness of the layer d, providing the formation of such a regime for arbitrary polarization and wavelength λ by using the following expression derived from Eqs. (21) and (18):

$$\frac{d}{\lambda}=\frac{\sqrt{1-4(1-\gamma)^2}\arccos(m)}{2\pi n_0}. \tag{40}$$

Thus, for the set of parameters related to Fig. 2 and $\lambda=1.55$ μm, Eq. (40) defines the thickness of the layer $d=45$ nm; herein Fig. 2 remains valid for any values of d and λ, linked by relation (40) with $m=0.75$, $n_0=3.4$, and $\gamma=0.75$.

To compare these results with the transmittance of an homogeneous layer ($m=1$) with the same values of d and n_0, one can use the formulas for reflection coefficients R_s and R_p [20], presented in forms similar to that of Eqs. (31) and (37), respectively,

$$R_s=A_s(B_1+iB_2)^{-1},\quad A_s=(n_0^2-1)tg\,\delta,$$

$$B_1=(r^2+\cos^2\theta)tg\,\delta,\ B_2=2r\cos\theta,$$

$$r^2=n_0^2-\sin^2\theta,\quad \delta=\frac{\omega dr}{c}=\frac{2\pi n_0 d}{\lambda}\sqrt{1-\frac{\sin^2\theta}{n_0^2}},$$

$$R_p=A_p(B_3+iB_4)^{-1},\quad A_p=-(n_0^4\cos^2\theta-r^2)tg\,\delta,$$

$$B_3 = (n_0^4 \cos^2\theta + r^2) tg\,\delta, \quad B_4 = 2n_0^2 r \cos\theta. \tag{41}$$

For normal incidence ($\theta=0$) these formulas reduce to the natural result, $R_s=-R_p$. The transmittances $|T_s|^2$ and $|T_p|^2$, are then found by means of Eq. (39), and are also presented in Figs. 2, 3(a), and 3(b). To calculate the dependence of the transmittances on the frequency-dependent parameter $\gamma(u)$, one needs to evaluate the factor $tg(\delta)$ by using the ratio d/λ, as a function of $\gamma(u)$ and that is given by Eq. (40). The spectral properties of transmittance for S and P waves are presented in Figs. 3–6 in the $[|T|^2-\gamma(u)]$ or in the $[|T|^2-u]$ planes.

These graphs illustrate the quantitative differences in transmittances, produced by profiles $U(z)$. Namely, Fig. 3(b) shows a narrow spectral window for the total transmittance of S waves, which profoundly differs from the smoothly varying function $|T_s|^2$ for the homogeneous film. Herein the comparison of Figs. 3(a) and 3(b), drawn for one gradient layer, shows that the increase of depth of modulation of refractive index m can result in significant changes of the transmittance-reflection spectra of the gradient layer for S waves. A narrow asymmetrical peak of reflectionless tunneling for S waves arises near the point $u=1$, $\gamma=1$. This peak is contiguous with a narrow area of high dispersion of transmittance coefficient with almost vertical tangent to the graph $|T_s(\gamma)|^2$. The transmittance $|T_p|^2$ in this range remains almost constant, approximately 87%. When the angle of incidence is decreased the existence of the peak is unaffected while transmittance $|T_p|^2$ tends to 100% [see Fig. 3(c)].

On the other hand, in the lower-frequency spectral range close to the point $\gamma=0.5$—see Fig. 3(c)—the reflection of S waves is almost unvariable, close to 100%, while the transmittance of P waves tends to zero; herein the frequency dispersion of $|T_p|^2$ in this range is strong. The large contrast between the transmittance of gradient layers for S and P waves may prove to be of interest for polarizing systems, operating under the large angles of incidence. The thickness of the layers may be rather small: e.g., a polarizing screen, providing for transmitted waves the ratio $|T_p|^2/|T_s|^2<0.05$, is characterized, under the conditions shown in Fig. 3(c) ($u=3.2$), by the ratio $d/\lambda=0.025$ determined from Eq. (40). Such a miniaturized scale d represents a remarkable feature of the anisotropic gradient nanolayers considered.

IV. NARROW-BAND REFLECTIONLESS TUNNELING OF S WAVES

While discussing the transmittance peaks for S waves $|T_s|^2=1$ in the spectral range $\gamma(u)\leqslant 1$ [Figs. 3(b) and 3(c)], one has to emphasize that these peaks arise in the regime of the reflectionless tunneling of wave ($R_s=0$) through the gradient layer. The cancellation of the reflected-wave results from the interference of the wave reflected on the interface $z=-d/2$, with the transmitted part of the backward antievanescent wave. This cancellation arises only for the concave photonic barrier: in the case of a square barrier with a constant refractive index, such cancellation proves to be impossible [17].

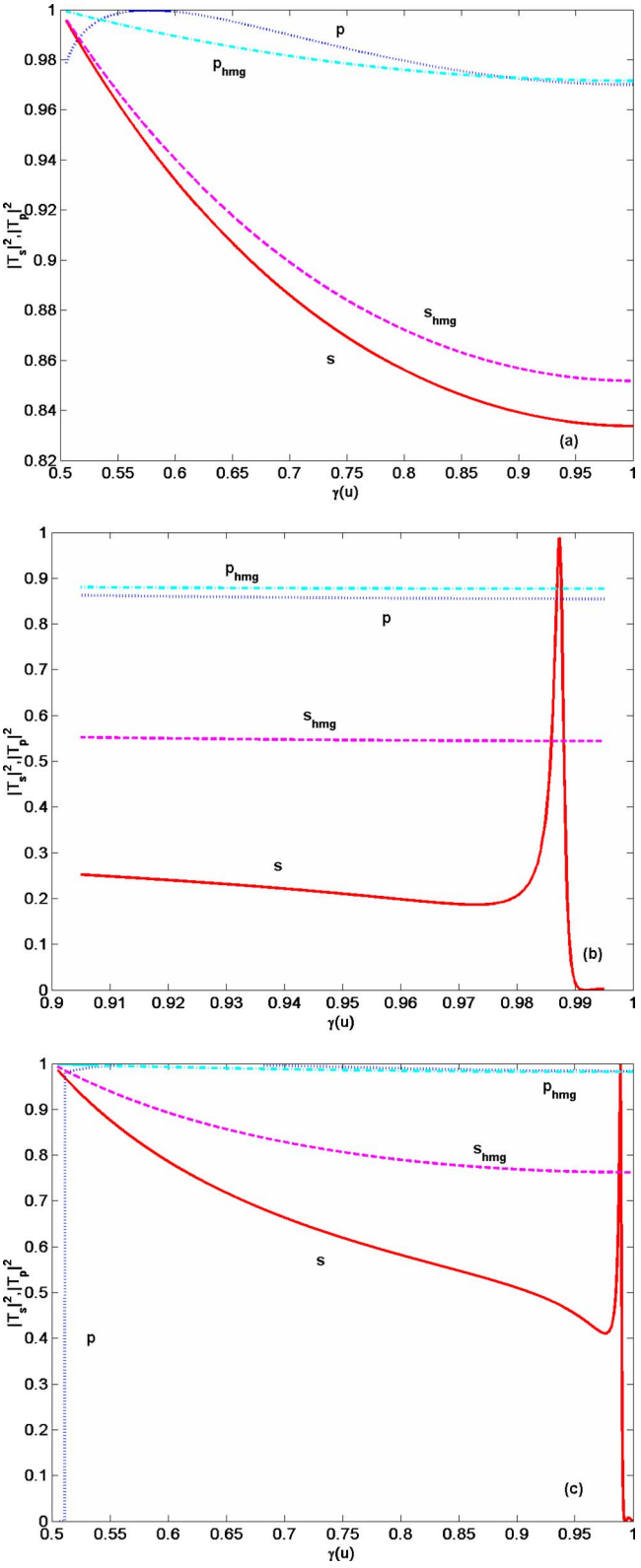

FIG. 3. (Color online) Spectra of the transmittance of both the gradient and homogeneous single layer ($n_0=1.4$) for the inclined incidence of S (full line) and P waves (dotted line) vs the frequency-dependent parameter $\gamma(u)$ [Eq. (21)]; (a) $m=0.95$, $\theta=75°$; (b) $m=0.75$, $\theta=75°$; (c) $m=0.75$, $\theta=65°$. Transmittances associated with the homogeneous layer for the S and the P wave are indicated by the dashed and the dash-dotted line, respectively.

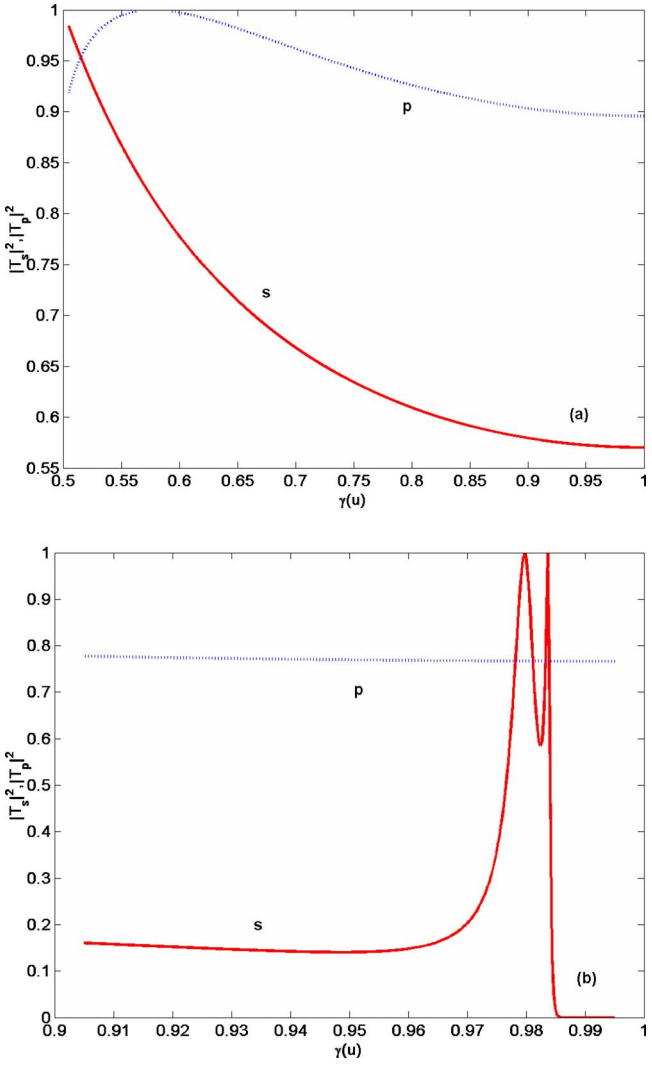

FIG. 4. (Color online) Spectra of the transmittance of a pair of layers (n_0=1.4, θ=75°) for the S (full line) and the P waves (dotted line). (a) m=0.95;(b) m=0.86.

Proceeding in a similar fashion, we can find the transmittance of a pair of gradient layers for S- and P-polarized waves, characterized by coefficients $|T_{2s}|^2$ and $|T_{2p}|^2$. To calculate these coefficients let us examine the set of two parallel adjacent layers, shown in Fig. 1. Herein the continuity conditions on the interfaces $z=-d/2$ and $z=3d/2$ remain unchanged. Considering first the S wave, one can see that formulas for R_s [Eq. (28)] and Q_s [Eq. (30)] relating to these conditions for the S wave, are also valid for the set of two layers. Recalling these conditions for the intermediate boundary $z=d/2$, one can find, after some tedious algebra, the value Q, related to this boundary,

$$Q = -\left[\frac{F_1M_2 + M_1F_2 + 2Q_sM_2F_2}{Q_s(F_1M_2 + M_2F_1) + 2M_1F_1}\right]. \tag{42}$$

Here the values $M_{1,2}$ and Q_s are defined in Eqs. (29) and (30). The substitution of Eq. (42) into Eq. (28) yields the complex reflection coefficient R_{2s} for the set of two layers,

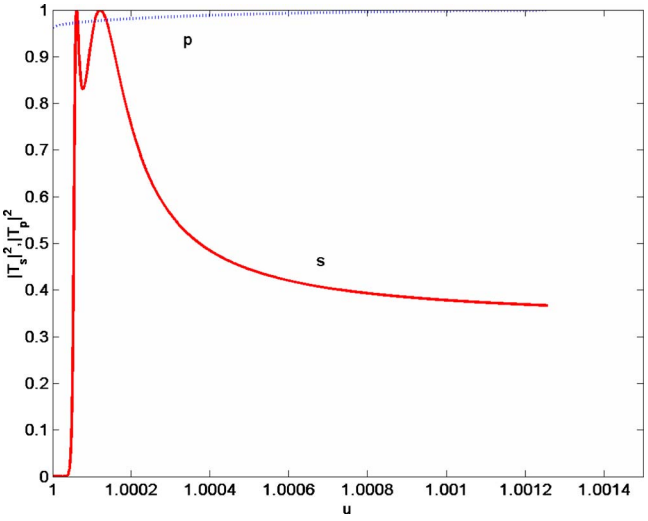

FIG. 5. (Color online) Narrow-band peaks of the reflectionless tunneling of S (full line) and P waves (dotted line) through the pair of gradient layers (n_0=1.4, m=0.75, θ=65°). The transmission coefficients are plotted vs the normalized frequency u.

$$R_{2s} = \frac{G_s}{K_s + iJ_s},$$

$$G_s = (F_1M_1 - F_2M_2)[M_1^2 - M_2^2 + \zeta_s^2(F_1^2 - F_2^2)],$$

$$K_s = (F_1M_1 - F_2M_2)[M_2^2 - M_1^2 + \zeta_s^2(F_1^2 - F_2^2)],$$

$$J_s = \zeta_s[(F_1^2 - F_2^2)(M_1^2 - M_2^2) + (F_1M_1 - F_2M_2)^2]. \tag{43}$$

The reflection coefficient of the same pair for the P wave R_{2p} can be determined by analogy with Eq. (43) by means of the replacement of indices $s \to p$ in the relevant terms in Eqs. (42) and (43), e.g., $G_s \to G_p$, and the following transpositions:

$$R_{2p} = \frac{G_p}{K_p + iJ_p},$$

$$F_{1,2} \to F_{3,4}, \quad M_{1,2} \to M_{3,4}, \quad \zeta_s \to \zeta_p. \tag{44}$$

In the case of normal incidence one again obtains $|R_{2s}|^2 = |R_{2p}|^2$ (see the Appendix).

The transmission coefficients $|T_{2s}|^2$ and $|T_{2p}|^2$ for the pair of layers, found by means of the substitution of Eqs. (43) and (44) into Eq. (39), are presented in Fig. 4. The comparison of Figs. 4(a) and 4(b) shows the strengthening of optical anisotropy of gradient films due to the increase of their heterogeneity. The decrease of m from m=0.95 [Fig. 4(a)] to m =0.86 [Fig. 4(b)] results again in the formation of reflectionless tunneling (nonattenuated transmittance) regimes for S waves as well as the huge dispersion of $|T_{2s}|^2$ and the slowly varying high transmittance of P waves near the point u=1. However, in this geometry the range of reflectionless tunneling contains two closely located peaks with a very narrow spectral width (see Fig. 5). Thus, such a pair of films can be considered as a model of miniaturized frequency filter for S waves. We note that the effects of nonattenuated tunneling

analogous to the superlensing phenomenon in which evanescent waves contribute to the perfect image of the objects by means of negative refractive index medium [18], represent an alternative and new concept of energy transfer that employs evanescent waves and may be useful in the design of subwavelength devices.

In Fig. 6 we present the phase shifts of transmitted waves ϕ. The phase times $t_{ph}=\partial\phi/\partial\omega$ are positive for the S wave in all the spectral range $\gamma(u)<1$, while for the P wave the values t_{ph} are positive in a broad spectral interval $0.55<\gamma<1$ and negative in a narrow spectral interval $0.52<\gamma<0.55$. In the former interval the phase shift of P waves, passing through the pair of layers, can reach values close to $\pm\pi/2$.

A comparison of phases of reflected [Eq. (32)] and transmitted [Eq. (34)] S waves leads to the relation $tg\phi_{sr}tg\phi_{st}+1=0$. A similar relation between the phases can be found from Eqs. (37) and (38) for P waves as well, and they are linked as

$$\phi_{sr}-\phi_{st}=\phi_{pr}-\phi_{pt}=\pm\frac{\pi}{2}. \tag{45}$$

Formulas (43) and (44) show that the correlation (45), derived for one layer, remains valid for a pair of layers. This property can be used for the determination of the phase of tunneling wave, if its detection is impeded due to strong attenuation in an opaque barrier [19].

Until now our analysis was restricted to the model of heterogeneous films without a substrate. To examine the applicability of our results to the real case of a layer supported by a substrate, let us consider a layer deposited on an homogeneous lossless layer of thickness D and with refractive index n_D (see Fig. 1). By presenting the generating function for, e.g., the S wave, inside the homogeneous layer in the form

$$\psi_D=[\exp(ik_\perp z)+Q_D\exp(-ik_\perp z)]\exp[i(k_y y-\omega t)],$$

$$k_\perp=\frac{\omega}{c}r,\quad r=\sqrt{n_D^2-\sin^2\theta}, \tag{46}$$

and by using the continuity conditions on the interface between this layer and air ($z=d+D$), one can find the parameter Q_D that enters Eq. (46) in the form

$$Q_D=-\left(\frac{\cos\theta-r}{\cos\theta+r}\right)\exp(2ik_\perp D). \tag{47}$$

The continuity conditions on the interface between the layer and the heterogeneous film can be written by means of Eqs. (25)–(27).

$$\frac{M_2+Q_sM_1}{F_2+Q_sF_1}=\frac{2i\omega Lrm}{c}\left(\frac{1-Q_D}{1+Q_D}\right). \tag{48}$$

The expression in parentheses in Eq. (48) can be rewritten by means of Eq. (47) in the form

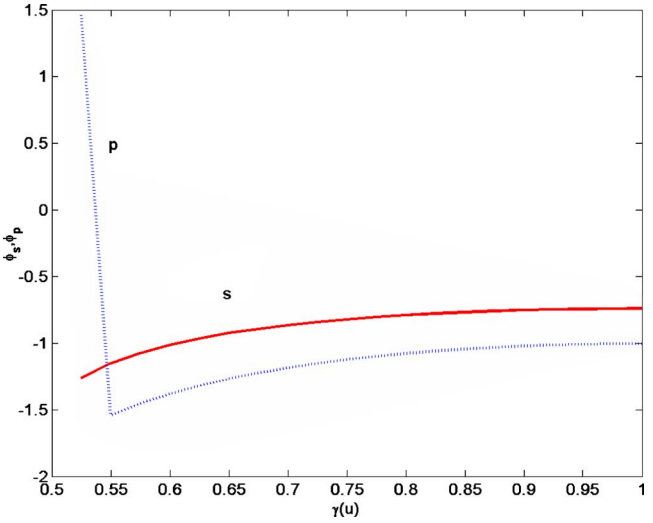

FIG. 6. (Color online) Phases of S (full line) and P waves (dotted line), propagating through the pair of layers under the conditions, given in the caption to Fig. 4(a).

$$\frac{1-Q_D}{1+Q_D}=\frac{\cos\theta-irtg\xi}{r-i\cos\theta},\quad \zeta=\frac{\omega rD}{c}. \tag{49}$$

If the thickness D is chosen so that

$$\frac{\omega D\sqrt{n_D^2-\sin^2\theta}}{c}=l\pi,\quad l=1,2,3,\ldots, \tag{50}$$

where the right side of Eq. (48) is reduced to $i\zeta_s$ [Eq. (29)], and the value Q_s, defined from Eq. (48), as well as the reflection coefficient R_s, coincide with the values (30) and (32), calculated in the absense of a substrate. The same condition (50) can also be found for the P wave. Thus, when the condition (50) is fulfilled, this layer does not affect the reflection-refraction properties of the gradient films discussed.

When the gradient layer is deposited on a homogeneous transparent substrate with refractive index n and thickness D, the expressions for reflection coefficients R_s and R_p obtained above can be generalized by means of the relevant continuity conditions on the interface $z=d/2$. In particular, in the case when $D\gg ct$, where t is the duration of the incident wave pulse (thick substrate)—so that no interference effects can occur between the incident and the far-interface reflected pulse—or when the reflection is eliminated by the use of an antireflection coating or by using a wedged substrate, these generalized expressions for a single layer read as

$$R_s=\frac{A_{s1}}{B_{s1}},$$

$$A_{s1}=M_1^2-M_2^2+\zeta_s\zeta_1(F_1^2-F_2^2)+i(\zeta_s-\zeta_1)(F_1M_1-F_2M_2),$$

$$B_{s1}=M_2^2-M_1^2+\zeta_s\zeta_1(F_1^2-F_2^2)+i(\zeta_s+\zeta_1)(F_1M_1-F_2M_2),$$

$$\zeta_1=\zeta_s\frac{r}{\cos\theta},$$

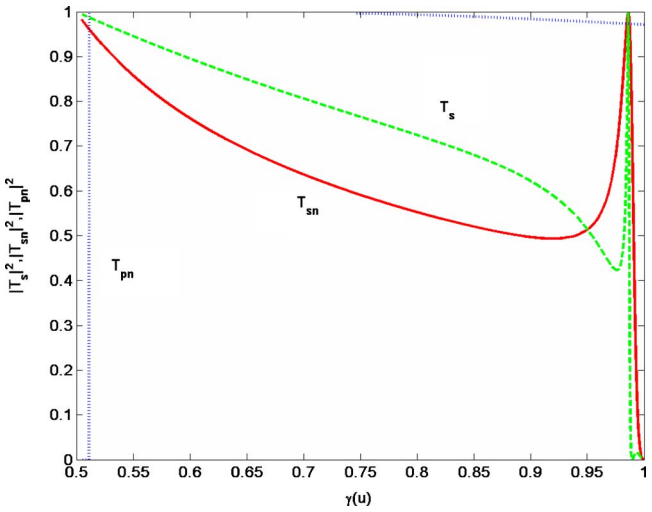

FIG. 7. (Color online) Transmittance of S (full line) and P waves (dotted line) propagating through one layer gradient photonic barrier denoted by T_{sn} and T_{pn}, respectively, deposited on the thick substrate with $n=2.32$ ($m=0.86$, $\theta=65°$, $n_0=1.4$); the curve indicated by T_s (dashed line) shows the transmittance of the same barrier without a substrate.

$$r = \sqrt{n^2 - \sin^2\theta}. \tag{51}$$

The value R_p can be obtained from this R_s by applying the transpositions

$$A_{s1} \to A_{p1}, \quad B_{s1} \to B_{p1}, \quad F_{1,2} \to F_{3,4}, \quad M_{1,2} \to M_{3,4},$$

$$\zeta_s \to \zeta_p, \quad \zeta_1 \to \zeta_p \frac{r}{\cos\theta}.$$

In the case when $n=1$ (air) and $r=\sin\theta$, these formulas reduce to Eqs.(31) and (37), respectively. The condition of reflectionless tunneling $R_{1s}=0$ results in two equations, nullifying the real and imaginary parts of the numerator A_{s1}. Combining Equations $\mathrm{Re}[A_{s1}]=0$, and $\mathrm{Im}[A_{s1})]=0$, one obtains the expression r,

$$\frac{r}{\cos\theta} = \frac{M_2^2 - M_1^2}{\zeta_s^2(F_1^2 - F_2^2)}. \tag{52}$$

The right side of Eq. (52) is known, therefore $r = \sqrt{n^2 - \sin^2\theta}$ and, finally, one obtains the value of the refractive index of substrate n, which provides such nonattenuated tunneling. Then the values T_s and T_p can be calculated by using Eq. (39). An example of transmittance through a gradient photonic barrier deposited on a thick substrate with refractive index n for the S and P waves, calculated according to Eq. (52), is depicted in Fig. 7 and denoted by T_{sn} and T_{pn}, respectively. We find that the presence of the thick substrate affects the transmittance for the S wave (denoted by T_s in Fig. 7) and results in a broadening of the peak of the transmittance and an increase of its minimum in comparison with the transmittance without the substrate. However, the main tendencies in the spectrum remain unchanged, while the change of the transmittance for the P wave is negligible.

V. CONCLUSIONS

In conclusion, we have considered the transmittance of gradient photonic barriers, formed by thin dielectric layers with concave profiles of refractive index, for both S- and P-polarized EM waves, incidenting on these barriers under arbitrary angles. The nonlocal dispersion, determined by the shape of photonic barriers, is shown to provide a peculiar optical anisotropy, stipulating the propagation of the P (S) -polarized waves in the traveling (tunneling) regime. The amplitude-phase structure of reflected and transmitted S- and P-polarized waves is found in the framework of the exactly solvable model of gradient barriers, and the generalized Fresnel formulas for the reflectance and transmittance of single-layer and double-layer concave photonic barriers are presented. The effect of narrow-band reflectionless tunneling (100% transmittance) of the S wave is demonstrated. These solutions, obtained without any assumptions regarding the smallness or slowness of variations of EM fields or media, can be used as a benchmark of some approximations, found by the transfer-matrix approach [20] or numerical solutions for EM fields in spatially varying media [21]. The examples of the use of these results in the gradient optics of nanolayers may become useful for the design of miniaturized subwavelength optoelectronic devices, operating with the oblique incidence of EM waves, such as polarizers, phase shifters, frequency-selective interfaces, and large incidence angles filters.

In the optical and near IR domain, there are already known technological solutions to the fabrication of such devices. Gradient index films with refractive index variations in excess of 30%—typically 1.45–1.9—over a few tens of nanometers can be realized using, e.g., silicon oxinitride with varying O/N stoichiometry [22]. The plasma enhanced chemical vapor deposition technology used in the fabrication of such structures allow large-scale treatment. The Ion-implantation method represents another solution for controlling locally the refractive index of a material.

If the methods used for obtaining such gradient layers can be generalized to materials operating in different wavelength ranges, the scalability of our exact analytical solutions to the different spectral ranges opens new perspectives for the design of materials with electromagnetic properties unattainable in the natural media.

ACKNOWLEDGMENTS

One of the authors (A.S.) acknowledges the stimulating discussions with Professor T. Arecchi and A. Migus. A.S and G.P. acknowledge the support of NATO (Grant No. PST.CLG 980331). The work of V.K. was partially supported by the COST P11 Action.

APPENDIX

To confirm the equality of fields inside the barrier and of the reflection coefficients for S and P waves in the case of normal incidence ($k_y=0$, $d/dy=0$), let us start from general Eq. (2) for the S wave and Eq. (4) for the P wave; with an incidence angle tending to zero, these equations coincide if

$$E_{xs} = E_{yp}, \quad H_{ys} = -H_{xp}. \tag{A1}$$

To verify that the solutions obtained above from different equations for S and P waves, satisfy these conditions, one needs to (1) establish the link between the generating functions Ψ_s and Ψ_p in the case of normal incidence; (2) find the expressions for the field components for S and P waves, this link being taken into account; and (3) compare these expressions, revealing their coincidence. These steps are performed below.

(1) In the case of normal incidence, Eq. (8) for the P wave can be viewed as resulting from the differentiation of Eq. (7) for the S wave with respect to z; i.e.,

$$\Psi_p = \frac{d\Psi_s}{dz} \tag{A2}$$

and, thus, generating functions Ψ_s and Ψ_p for this case are not independent.

(2) A generating function for S waves Ψ_s inside the film can be presented as a sum of forward and backward waves [Eq. (23)],

$$\Psi_s = A[\Psi_{s1}(z) + Q_s\Psi_{s2}(-z)]. \tag{A3}$$

Here A is a constant and Q_s determines the contribution of the backward wave to the total field. The substitution of Eq. (A3) into Eq. (5) brings the electric and magnetic components of the S wave. Introducing the quantities

$$\frac{d\Psi_{s1}(z)}{dz} = (\Psi_{s1})', \quad \frac{d\Psi_{s2}(-z)}{dz} = -(\Psi_{s1})', \tag{A4}$$

where the notation $(\Psi)'$ indicates the derivative of function Ψ with respect to its argument, and using the relation (A2), one can write by means of Eq. (5),

$$E_{xs} = \frac{i\omega}{c}\Psi_s, \quad H_{ys} = A[(\Psi_{p1} - Q_s\Psi_{p2})]. \tag{A5}$$

We point out that the H_{ys} component is expressed here via the generating function of the P wave. On the other hand, considering the generating function for the P wave in a form, similar to Eq. (A3),

$$\Psi_p = B[\Psi_{p1}(z) + Q_p\Psi_{p2}(-z)], \tag{A6}$$

one obtains by substituting Eq. (A6) into Eq. (6),

$$H_{xp} = -\frac{i\omega B}{c}[\Psi_{p1}(z) + Q_p\Psi_{p2}(-z)]. \tag{A7}$$

Now let us write the expression for E_p [Eq. (6)] in the form

$$E_{yp} = \frac{B}{n_0^2U^2}[(\Psi_{p1})' - Q_p(\Psi_{p2})'], \tag{A8}$$

where B is some constant. Using Eq. (A2), one can express the first derivative of Ψ_{p1} via the second derivative of Ψ_{s1}: $(\Psi_{p1})' = (\Psi_{s1})''$, as well as $(\Psi_{p2})' = (\Psi_{s2})''$; presenting these second derivatives by means of Eq. (7), governing the generating function Ψ_s for normal incidence, one obtains from Eq. (A8),

$$E_{yp} = -\frac{\omega^2}{c^2}B(\Psi_{s1} - Q_p\Psi_{s2}). \tag{A9}$$

Thus, the component E_p of the P wave proves to be expressed via the generating function for the S wave. Now one has to compare the values H_s and H_p as well as E_s and E_p, revealing the link between Q_s and Q_p in the case $k_y=0$. One can use the general properties of hypergeometric functions [16],

$$F(\alpha,\beta,\gamma,v) = 1 + \frac{\alpha\beta}{\gamma}v + \cdots,$$

$$\frac{dF}{dv} = \frac{\alpha\beta}{\gamma}F(\alpha+1,\beta+1,\gamma+1,v),$$

$$v(1-v)\frac{dF(\alpha,\beta,\gamma,v)}{dv} = (\gamma-\alpha)F(\alpha-1,\beta,\gamma,v) - (\gamma-\alpha-\beta v)F(\alpha,\beta,\gamma,v). \tag{A10}$$

The values of parameters α and β for S and P waves for the normal incidence are found from Eqs. (22) and (36), respectively,

$$\alpha_s = \beta_s = \frac{1-N}{2}, \quad \alpha_p = \frac{3-N}{2}, \quad \beta_p = -\left(\frac{1+N}{2}\right). \tag{A11}$$

The product $v(1-v)$ in Eq. (A1), calculated for the planes $z=\pm d/2$, is equal to $m^2/4$. Parameters $M_{1,2}$ [Eq. (29)] and $M_{3,4}$ [Eq. (37)] can be rewritten by means of Eqs. (A10)–(A12) as

$$M_1 = (1-N)F_3, \quad M_2 = -(1-N)F_4,$$

and

$$M_3 = -(1+N)F_1, \quad M_4 = (1+N)F_2. \tag{A12}$$

Now one can use Eq. (12) for transformation of the aforesaid factors Q_s [Eq. (30)] and Q_p [Eq. (35)]. Dividing both the numerator and denominator of Eq. (30) by the quantity $i\zeta_s$, and using the link between ζ_s [Eq. (29)] and ζ_p [Eq. (35)], arising in a case $\theta=0$,

$$\frac{1-N}{\zeta_s} = \frac{\zeta_p}{1+N}, \tag{A13}$$

and using the relations (A12), one obtains the link between Q_s and Q_p in the case discussed,

$$Q_p = -Q_s. \tag{A14}$$

The substitution of Eq. (A14) into the expression for H_p [Eq. (A7)] yields the link between free parameters A and B,

$$A = \frac{i\omega B}{c}, \tag{A15}$$

providing the fulfillment of condition $H_{xp}=-H_{ys}$ [Eq. (A1)]. The substitution of Eqs. (A14) and (A15) into the expression

for E_{yp} [Eq. (A9)] and then comparing with E_s [Eq. (A5)] shows that condition $E_{xs}=E_{yp}$ [Eq. (A1)] is fulfilled too.

Thus, the field components determined by means of generating functions Ψ_s and Ψ_p, governed by Eqs. (7), (8), and (15)–(17), and those ones, governed directly by Maxwell equations (2) and (4), coincide for the normal incidence. Moreover, the substitution of Eq. (A12) into the formula for R_s [Eq. (31)] and a comparison with R_p [Eq. (37)] yields finally the physically clear result for normal incidence on the gradient layer,

$$R_p = -R_s, \quad |T_s|^2 = |T_p|^2. \tag{A16}$$

The same substitution into the expression (43) for R_{2s} yields the similar results for normal incidence on a pair of layers,

$$R_{2p} = -R_{2s}, \quad |T_{2s}|^2 = |T_{2p}|^2. \tag{A17}$$

Thus, in case of normal incidence, the difference between the solutions for S and P waves is vanishing; the regime of propagation in the gradient layer in this case is the same for both waves.

[1] G. Gamow, Z. Phys. **51**, 204 (1928).
[2] D. Marcuse, *Theory of Dielectric Optical Waveguides* (Academic, New York, 1990).
[3] E. Moritz, Mol. Cryst. Liq. Cryst. **41**, 63 (1977).
[4] A. Snyder and D. Mitchell, Electron. Lett. **9**, 609 (1973).
[5] A. M. Shaarawi, B. T. Tafwik, and I. M. Besieris, Phys. Rev. E **62**, 7415 (2000).
[6] Chun-Fang Li and Qi Wang, J. Opt. Soc. Am. B **18**, 1174 (2001).
[7] A. Ranfagni, P. Fabeni, G. Pazzi, and D. Mugnai, Phys. Rev. E **48**, 1453 (1993).
[8] A. Haibel, G. Nimtz, and A. Stahlhofen, Phys. Rev. E **63**, 047601 (2001).
[9] F. Fornel, *Evanescent Waves: From Newtonian Optics to Atomic Optics*, Springer Series in Optical Sciences Vol. 73 (Springer, Berlin, 2001).
[10] T. E. Hartman, J. Appl. Phys. **33**, 3427 (1962).
[11] V. S. Olkhovsky, E. Recami, and J. Jakiel, Phys. Rep. **398**, 133 (2004).
[12] P. Yeh, *Optical Waves in Layered Media*, Wiley Series in Pure and Applied Optics (Wiley, New York, 1997).
[13] Ph. Balcou and L. Dutriaux, Phys. Rev. Lett. **78**, 851 (1997).
[14] V. Laude and P. Tournois, J. Opt. Soc. Am. B **16**, 194 (1999).
[15] A. Shvartsburg and G. Petite, Eur. Phys. J. D **36**, 111 (2005).
[16] M. Abramowitz and I. Stegun, *Handbook of Mathematical Functions* (Dover, New York, 1968).
[17] A. Shvartsburg and G. Petite, Opt. Lett. **31**, 1127 (2006).
[18] J. B. Pendry, Phys. Rev. Lett. **85**, 3966 (2000).
[19] C. K. Carniglia and L. Mandel, J. Opt. Soc. Am. **61**, 1035 (1971).
[20] D. J. Griffiths, *Introduction to Electrodynamics* (Prentice-Hall, Englewood Cliffs, NJ, 1999).
[21] S. Menon, Q. Su, and R. Grobe, Phys. Rev. E **67**, 046619 (2003).
[22] A. Hofrichter, P. Bulkin, and B. Drevillon, Appl. Surf. Sci. **142**, 447 (1999).